Contribution from the Department of Chemistry and The James Franck Institute, The University of Chicago, Chicago, Illinois 60637

Pair Potentials, Electron-Pair Repulsions, and the Geometries of Molecules

Jeremy K. Burdett* and Thomas F. Fässler

Received November 9, 1990

The utility of a new parameter, the ligand–ligand pair potential, ϕ, and its variation with electron count (x) is used to understand the geometries of small molecules and the origin of electron-counting rules. Although derived from molecular orbital calculations and defined as representing the potential between pairs of atoms coordinated to a central atom, phenomenologically ϕ equally well represents the interactions between the *electron pairs* linking these atoms to the central one. This provides a way to extract an electron-pair repulsion picture from a one-electron molecular orbital theory and is able to provide some insights into why the VSEPR scheme works. We show how knowledge of the sign and magnitude of ϕ determines angular geometries, relative bond lengths, and critical electron counts for the electronic stability of molecules with certain structures. In contrast to the ideas of the VSEPR scheme, the model is equally applicable to main-group and transition-metal systems.

Introduction

Chemists have constantly sought new ways to understand the details of molecular geometry, and many different theoretical methods, varying in sophistication, have been used over the years to study the shapes of small molecules.[1] The molecular orbital based models initiated by Mulliken[2] and further developed by Walsh[3] in his classic series of papers have found an effective proponent in the Hoffmann school.[4] The ideas of Jahn and Teller[5] expanded to include pseudo- and second-order variants[6] have been of especial interest to transition-metal chemists. A recent advance has been the development of topological ideas,[7] via the method of moments, which has provided a global orbital picture. However, perhaps the most often used approach for main-group-centered molecules and solids is not a molecular orbital one at all but is the scheme developed over the years by Sidgwick, Powell, Nyholm, and Gillespie known as the valence-shell electron-pair repulsion (VSEPR) model.[8] Here the electron pairs around the central atom repel each other (supposedly by "Pauli" forces), and the equilibrium angular geometry arises via minimization of such interactions. The lengths of symmetry-inequivalent bonds are also set by repulsions between pairs of electrons. Irrespective of the theoretical justification of the model, it is certainly true that the geometries of small main-group molecles as mimicked by molecular orbital calculations behave as if there exist repulsions of this type between the electrons localized in the bonds. Bartell has exploited this result in his "points-on-a-sphere" approach,[9] and we have shown[10] using a molecular orbital model that the energetics of some four-electron-pair AX_4 species (where A is a main-group atom and X a typical ligand) behave as if the interbond potential scales as r^{-1}, exactly the functional form expected from Coulomb's law. The two types of model are based on diametrically opposite concepts. One-electron molecular orbital ideas concentrate on overlap forces and ignore electron–electron interactions, but the VSEPR scheme ignores overlap forces and concentrates on electron–electron interactions. In this paper, we examine the utility of a new parameter, the ligand–ligand pair potential, derived from molecular orbital calculations and defined as representing the potential between pairs of atoms coordinated to a central atom, but phenomenologically equally well representing the interactions between the *electron pairs* linking these atoms to the central one. This provides a way to extract an electron-pair repulsion picture from a one-electron molecular orbital theory.

The Pair Potential

Pair potentials, whether between atoms, stable molecules, or molecular fragments is a well-used concept in the study of surfaces.[11] The signs and magnitudes of the first, second, and higher neighbor potentials and their analogues, describing the energetics associated with clusters of three or more adsorbed atoms, crucially control the ordering patterns found for adsorbed species and the phase diagram describing surface structure. If the pair potentials between two molecules adsorbed on a metal surface are positive, then the two species will repel one another and in general a collection of such adspecies will keep as far apart as possible. If these potentials are attractive, then the adsorbed species will arrange themselves into a surface cluster where atoms or molecules are found on adjacent atoms. The concept of the pair potential, however, is not one that has been generally used in molecular chemistry, but there is no reason that it should not. If the calculated pair potential between two coordinated atoms or groups is large and positive, then, by analogy with this surface discussion, one result is that the two ligands will be forced apart, leading either to a large structural change or to ejection of one ligand from the coordination sphere. The latter process is expected if the pair potential is larger than the metal–ligand bond energy. If the pair potential is positive but rather small, then this may reflect rather modest structural changes. Clearly, if the pair potential is zero, then the geometry under consideration is stable for that electron count. The pair potential may be readily computed once we realize what it represents energetically. If two ligands (X, Y) have a zero pair potential, then this implies that the coordination of one is energetically independent of the presence of the other. This means that the bond energy associated with the attachment of X to a central atom (A) is the same irrespective of the coordination of Y. So, a useful operational definition of the pair potential (ϕ) between two ligands X in a complex of stoichiometry AX_n is just

$$\phi = 2[E(AX_n) - E(AX_{n-1})] - [E(AX_n) - E(AX_{n-2})] \quad (1)$$

which simply reduces to

$$\phi = [E(AX_n) + E(AX_{n-2})] - 2[E(AX_{n-1})] \quad (2)$$

Of course, depending upon the geometry of the molecule, several different pair potentials may be defined, including cis, trans, axial–equatorial, etc. We shall use one-electron ideas to explore the implications for this parameter and note that although the computation of a bond strength using such theories is usually a worthless endeavor, the total number of A–X linkages is the same

* To whom correspondence should be addressed at the Department of Chemistry.

(1) For example: Burdett, J. K. *Molecular Shapes*; Wiley: New York, 1980.
(2) Mulliken, R. S. *Rev. Mod. Phys.* **1942**, *14*, 204.
(3) (a) Walsh, A. D. *J. Chem. Soc.* **1953**, 2260, 2266, 2288, 2296, 2301, 2306. (b) Gimarc, B. *Molecular Structure and Bonding*; Academic Press: New York, 1979.
(4) For example: Hoffmann, R.; Elian, M. *Inorg. Chem.* **1975**, *14*, 1058.
(5) Jahn, H. A.; Teller, E. *Proc. R. Soc. London* **1937**, *A161*, 220.
(6) Bartell, L. S. *J. Chem. Educ.* **1968**, *45*, 754. Pearson, R. *J. Am. Chem. Soc.* **1969**, *91*, 1252.
(7) (a) Burdett, J. K.; Lee, S. *J. Am. Chem. Soc.* **1985**, *107*, 3050. (b) Burdett, J. K.; Lee, S. *J. Am. Chem. Soc.* **1965**, *107*, 3063. (c) Burdett, J. K.; Lee, S.; McLarnan, T. J. *J. Am. Chem. Soc.* **1965**, *107*, 3083. (d) Burdett, J. K. *Struct. Bonding (Berlin)* **1967**, *65*, 30.
(8) Gillespie, R. J. *Molecular Geometry*; Van Nostrand-Rheinhold: London, 1972. Gillespie, R. J.; Nyholm, R. S. *Q. Rev., Chem. Soc.* **1957**, *11*, 339. Gillespie, R. J. *Angew. Chem., Int. Ed. Engl.* **1967**, *6*, 819.
(9) Bartell, L. S. *J. Am. Chem. Soc.* **1973**, *95*, 3097. Bartell, L. S. *Croat. Chim. Acta* **1984**, *57*, 927.
(10) Burdett, J. K.; McLarnan, T. J. *Am. Mineral.* **1984**, *69*, 804.
(11) Einstein, T. L. In *Chemistry and Physics of Solid Surfaces*; Vanselow, R., Ed.; CRC Press: Boca Raton, FL, 1979. Einstein, T. L. *CRC Crit. Rev. Solid State Sci.* **1978**, *7*, 260.

0020-1669/91/1330-2859$02.50/0

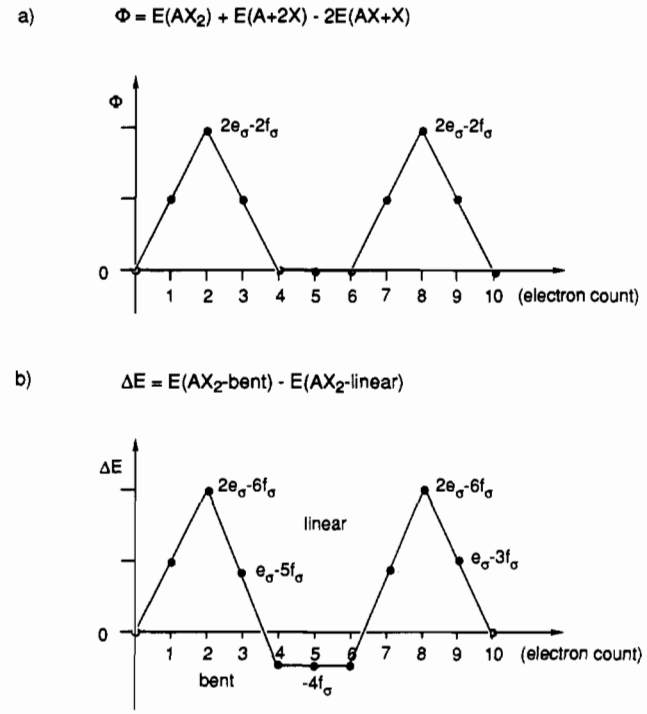

Figure 1. Pair potential and energy difference curves derived from the angular overlap model using p orbitals for the central atom A in AX_2 only as a function of electron count: (a) pair potential, ϕ, between the two ligands X for the bent molecule AX_2 (angle XAX = 90°); (b) energy difference curve ΔE for bent and linear AX_2.

for both bracketed expressions in eq 2. Calculation of the pair potential in this way is therefore expected to be a valid procedure. In Appendix I we describe further aspects of the calculation of ϕ. Of particular utility is the study of $\phi(x)$, the pair potential as a function of fractional orbital occupancy (empty, $0 < x < 1$, full). We recall the broader perspective obtained by viewing such electronic parameters as a function of electron count using some results from the method of moments.[7] Specifically, study of the behavior of the energy difference between two structures as a function of electron count, $\Delta E(x)$, has been particularly profitable.

As an illustration of the method, we show in Figure 1a the calculated value of the pair potential, $\phi(x)$, between the two X ligands for the bent AX_2 geometry obtained using this prescription. ($\phi(x)$ evaluated at the linear geometry is identically zero for all x.) Figure 1b shows the calculated energy difference curve $\Delta E(x)$ for the linear and bent molecules. The model used is probably the simplest possible and employs only the central atom p orbitals, two ligand orbitals, and the angular overlap model[1] to evaluate the orbital energies shown in Figure 2. As in the Rundle–Pimentel recipe,[12] two electrons are stored in the stereochemically impotent (on this model) central atom s orbital. The $\Delta E(x)$ plot has four nodes, just as expected on the basis of the moments method and described earlier in those terms.[7b] The predictions of the plot are in complete agreement with experiment and the geometries expected on the basis of VSEPR. Molecules with a total of four electrons (two in s, two in the set of orbitals used here) are expected to be linear (e.g. BeH_2), those with six and eight electrons (e.g. singlet CH_2 and OH_2, four and six electrons, respectively, in the p orbitals) are expected to be bent, and those with ten electrons (e.g. "NeH_2" or KrF_2, eight in the p orbitals) are expected to be linear again. These geometries are in excellent agreement with the predictions using the $\phi(x)$ plot for the two ligands in the bent geometry. $\phi(x)$ is large and positive for a total number of two (BeH_2) and five ("NeH_2") valence electron pairs (two and eight electrons, respectively, in the p orbitals), a result demanding opening of the XAX angle toward the linear geometry. For a total number of six (CH_2) and eight (OH_2) valence electrons, respectively (four and six electrons, respectively, in the p orbitals), $\phi(x)$ is identically zero, indicating stability of the bent geometry here. Thus there is a perfect match between the geometry predictions of the two plots.

Table I. The First Five Moment Differences for Linear and Bent Structures in Terms of the Interaction Integrals β and the Differences in Orbital Ionization Energies[a]

	1–3	4	5
p	0	$-4\beta_p^4$	$-10\beta_p^4\Delta n$
s+p	0	$-4\beta_p^4 + 8\beta_s^2\beta_p^2$	$(20\beta_s^2\beta_p^2 - 10\beta_p^4)\Delta m + (10\beta_s^2\beta_p^2 - 10\beta_p^4)\Delta sp$
d	0	$-16\beta_a^4\beta_b^2$	$-40\beta_a^2\beta_b^2\Delta l$

[a] Parameters correspond to Figure 4 and diagram 1.

It is appropriate at this stage to make a connection with VSEPR where the geometry is set by the repulsions between the various pairs of electrons in the form of bond pairs and lone pairs. The present model at face value leads to an explanation of the geometries of these molecules based on the variation with electron count of the repulsion between the two ligands X. But it is important to appreciate that this "repulsion" is not of the steric type. No orbital interactions between the ligands are included in the calculation, and thus their mutual influence has to be through the A–X bonds. We could thus equally well rephrase this explanation of the AX_2 molecular geometry problem in terms of the repulsion between the *electron pairs* in the A–X bonds. Such a description then leads to some obvious parallels with the tenets of the VSEPR scheme. However, with the use of VSEPR, the geometry beyond BeH_2 is set by repulsions between an increasing number of lone pairs and between these lone pairs and the bond pairs, but on the present model the geometry is set by variation with electron count of the magnitude of the "bond pair repulsions". The latter, for our simple example here, are associated purely with the p-orbital manifold, but in the VSEPR scheme they must include the valence s orbital pair. We note that an ab initio study[13] of the stereochemical importance of the 2s orbital on oxygen leads to the conclusion that the Rundle–Pimentel assumption is, in fact, probably quite correct here. The HOH angle in water (expected to be close to 90° on the Rundle–Pimentel scheme), rather than being the natural tetrahedral angle from VSEPR, is opened up from 90° by H···H interactions, a suggestion also made in ref 1. There is no consistent picture within the VSEPR framework for the angles found close to 90° in H_2S(e) and H_2Te.

AX_n and ML_n Systems

In this section we describe for a series of AX_n (where A is a main-group atom and X a typical ligand) and ML_n (where M is a transition metal and L a typical ligand) molecules the results of calculations of the extended Hückel type that lead to energy difference curves, $\Delta E(x)$, for pairs of structures and to pair potential plots, $\phi(x)$, for some selected atom pairs. One qualification has to be made at this stage. In order to present plots with some generality as a function of electron count, we used the same set of parameters irrespective of chemical identity. We mostly used a σ-only model, contracted the ligand orbital exponents (see Appendix II) to minimize overlap between the ligands, and kept all central atom–ligand distances fixed. Two sets of calculations are presented. In the first, s+p orbitals only are included for the central atom, and in the second, a d-orbital-only model is used. From the set of possible structures of main-group molecules and known transition-metal fragments, some selected for study are shown in Figure 3. For all pairs of structures, the first disparate moment in their energy density of states is the fourth, a result easily understood by counting the walks through the central atom as shown in Figure 3 and described in more detail elsewhere.[7] The energy difference curves as a function of x for each pair (Figure 4) should then have four nodes. This is however true only for the d-orbital model. From the calculations that employed s and p

(12) Rundle, R. E. *J. Am. Chem. Soc.* **1963**, *85*, 112. Rundel, R. E. *Surv. Prog. Chem.* **1963**, *1*, 81. Pimentel, G. C. *J. Chem. Phys.* **1951**, *19*, 446.

(13) Baird, N. C. *Inorg. Chem.* **1989**, *28*, 1224.

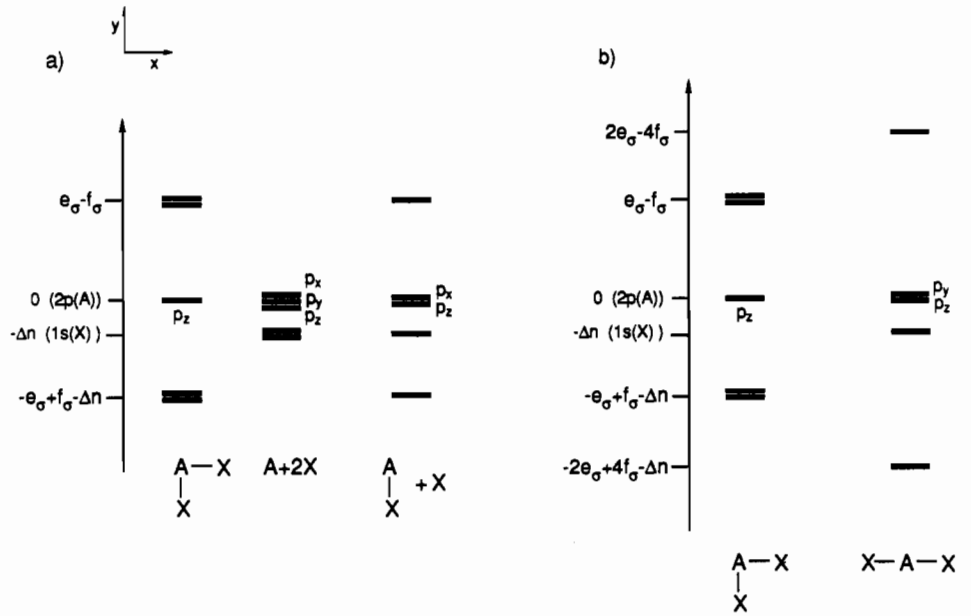

Figure 2. Molecular orbital diagrams for (a) bent AX_2 (central atom A with two nonbonding ligands X and AX with one nonbonding ligand X) and (b) bent and linear AX_2 using p orbitals for the central atom A and constructed with the angular overlap model. Δn is defined as $|H_{ii}(2p(A)) - H_{ii}(1s(X))|$.

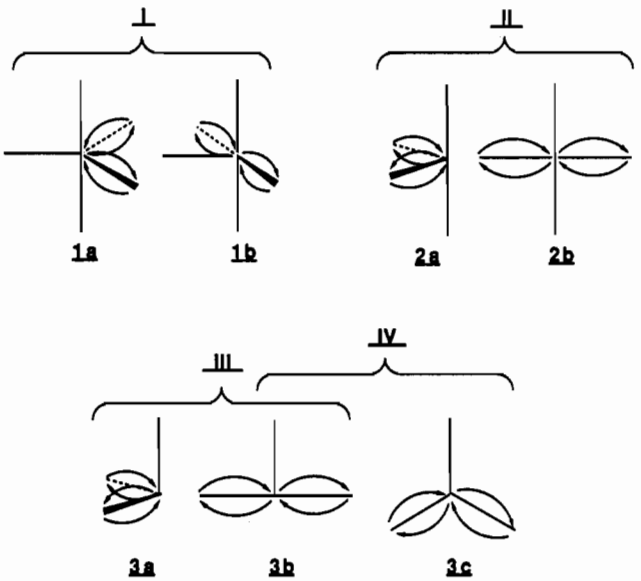

Figure 3. Possible structures of main-group molecules and transition-metal complexes of stoichiometries AX_5 (I), AX_4 (II), and AX_3 (III, IV) shown with the important walks of length 4.

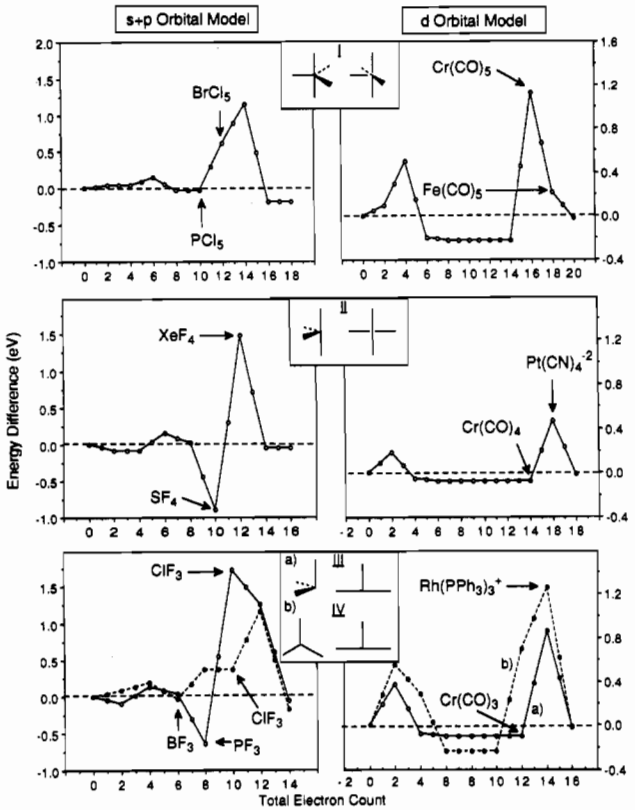

Figure 4. Calculated energy differences of pairs of AX_n and ML_n structures shown in **2** as a function of their electron count using s+p orbitals and d orbitals, respectively, for A and M and s orbitals only for X and L. Known examples with corresponding electron counts are indicated.

orbitals on the central atom, an additional node occurs in some of the plots. To understand its origin, it is profitable to study the linear versus bent AX_2 system. Table I and Figure 5 show the differences in n-walks, which lead to nth moment differences between the linear and bent molecules as a function of the model used (p-, s-, plus p-, and d-orbital models, respectively). The simplest way to visualize the state of affairs uses the p-only model. Allowing walks through p orbitals at A in AX_2 (Figure 5a), we see that there exist additional 4-walks in the linear system that are not possible in the bent one with an angle of 90°. This comes about simply because of the right angle between the two p orbitals. In the case where only d orbitals are used at the central A atom (Figure 5c), the walks have to be weighted by using the two different kind of overlaps ($\beta_a \propto \langle 1s|z^2\rangle$, $\beta_b \propto \langle 1s|x^2 - y^2\rangle$) in evaluating the first disparate moment.

The case where atom A holds both s and p orbitals (Figure 5b) is a little different. In order for the two ligand orbitals to "see" each other through A, a self-returning walk of length 4 is required of course. Only walks along bonds of length 4 occur in the fourth moment difference, and so there is no dependency on differences in ionization energy of the central atom s and p orbitals. Since there are no five-membered rings, such a dependence is found first at the fifth moment when walks in place may occur in addition to the walks along bonds. All fifth-moment difference terms contain one of the orbital energy differences shown in **1**. This is particularly important for the s+p orbital case, as we have described earlier.[7b] Notice that for this orbital model the difference in the fourth moment is zero for $\beta_s/\beta_p = (1/2)^{1/2}$. Thus, if the ratio of β_s to β_p is close to this value, then the fifth moment becomes important (and equals $-5\beta_p^4\Delta sp$ at the equality). The influence of the fifth moment is clear in a qualitative way in the

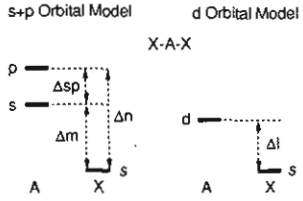

1

calculated results of Figure 4 for the pairs of structures II, III, and IV. In more general terms, we should expect that the geometries of these small molecules should be quite sensitive to the central atom s–p separation. We note that in fact that this has already been demonstrated. Hall[14] found by calculation a marked dependence of the geometries of these small molecules on this energy separation.

Figure 6 shows some pair potentials $\phi(x)$ for the set of molecules under consideration computed by using the same geometrical and electronic parameters used to generate Figure 4. They are shown for the chemically relevant part of x (see Appendix I) and mesh quite nicely with these $\Delta E(x)$ curves. All pairs of structures are related in the sense that the geometry with the smaller fourth moment can be transformed to the structure with a higher fourth moment by increasing the angle between two ligands as shown in **2**. In this moments language, for fourth-moment problems,

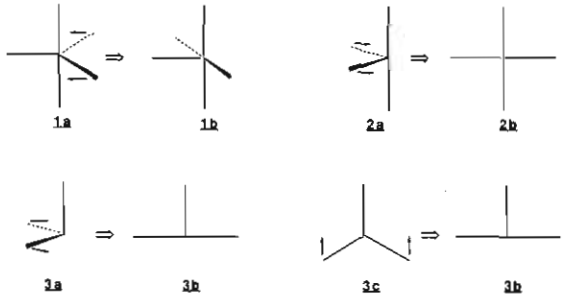

2

the resulting structures are generally energetically preferred at early and later orbital filling (Figure 4). Specifically, note how the equatorial–equatorial pair potential of the trigonal bipyramid is computed to be large and positive for $BrCl_5$ and the 16-electron species $Cr(CO)_5$. Opening this angle to 180° leads to the square-pyramidal geometry actually found for both of these molecules and the arrangement energetically preferred in Figure 4. (See ref 1 for the observed geometrical details of the molecules discussed here.) For PCl_5 and the 18-electron species $Fe(CO)_5$, the pair potential is positive but rather small, in keeping with the small energy difference calculated between these two structures at this electron count in Figure 4.

The computed results for PCl_5 and BCl_3 are interesting. Our $\phi(x)$ and $\Delta E(x)$ plots come from calculations where a generic set of orbital parameters have been used in an attempt at generality (Appendix II). However, they do not properly mimic the energetics associated with all molecules. Thus BCl_3 is predicted to be only just planar and PCl_5 only just trigonal bipyramidal from the $\Delta E(x)$ plot, whereas we would expect the energy differences to be somewhat larger. A study of different trigonal-bipyramidal molecules, with therefore different ligand orbital parameters, leads to changes in ΔE but little change in ϕ. ΔE for this set of calculations indicates a balance between ligand–ligand interactions and central atom–ligand forces in controlling the geometry.

The pyramidal geometry found experimentally for $Cr(CO)_3$ is well predicted by the zero pair potential for this geometry at d^6. The observed T-shape structure for d^8 $Rh(PPh_3)_3^+$ is in accord with the positive pair potential for both geometries. Notice the

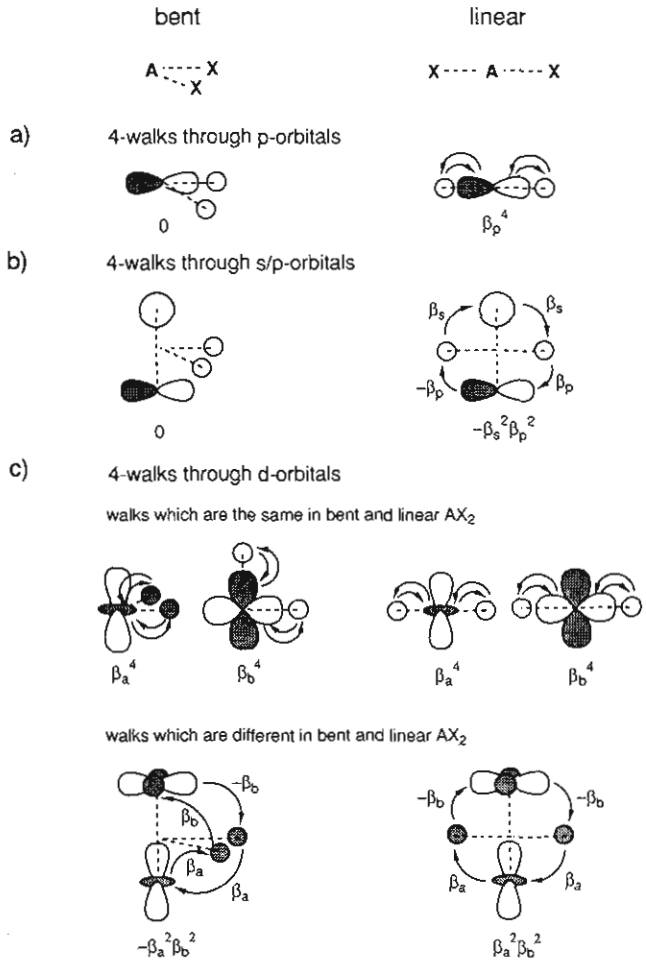

Figure 5. Walks through the central atom A of length 4 in bent and linear AX_n using (a) p-orbital, (b) s+p-orbital, and (c) d-orbital models for A. In (b) and (c) walks through two different orbitals located on atom A (s, p and $x^2 - y^2$, z^2, respectively) are shown.

larger value of ϕ for the geometry further away from the T. The trigonal-planar structure for d^{10} $Ni(CO)_3$ is in accord with the zero pair potential at this count.

For the series of four-coordinate molecules the positive pair potential found for the "octahedral cis-divacant" structure at 16 electrons in Figure 6 shows up as an energetic preference for the square-planar geometry in Figure 4. For the 14-electron $Cr(CO)_4$ molecule, this pair potential is zero, and the molecule is stable in this geometry. Exactly analogous comments apply to the pair of molecules XeF_4 and SF_4.

The pair potential calculated between cis ligands is a useful tool to examine angular geometry changes, but what are the properties of the pair potential between trans ligands? These forces, repulsive or attractive, will influence bond lengths only. A positive value of $\phi(x)$ should lead to a lengthening and a negative value to a shortening of these linkages relative to the others in the molecule. This is borne out in practice. Figure 7a shows the pair potential plot for trans ligands in geometries 2a and 3b (**2**) with maxima at 2 and 4 electrons, respectively, for the s+p orbital model. These electron counts correspond to the molecules SF_4 and ClF_3, which indeed have longer axial (for a description of these molecules based of a trigonal bipyramid) than equatorial bonds (SF_4 axial 164.6 pm, equatorial 154.5 pm; ClF_3 axial 169.8 pm, equatorial 159.8 pm). Similar results are found for a pair of the trans ligands that form the base of the square pyramid, geometry 1b. Here for the s+p-orbital model a strong positive pair potential between the two trans ligands is found at an electron count of 2 electrons. This would correspond to the longer equatorial than axial bond lengths actually found in BrF_5 (axial 168 pm, equatorial 175–182 pm). The lengthening of the axial bonds in molecules of geometry 1a (like PF_5) does not show

(14) Hall, M. B. *Inorg. Chem.* **1978**, *17*, 2261.

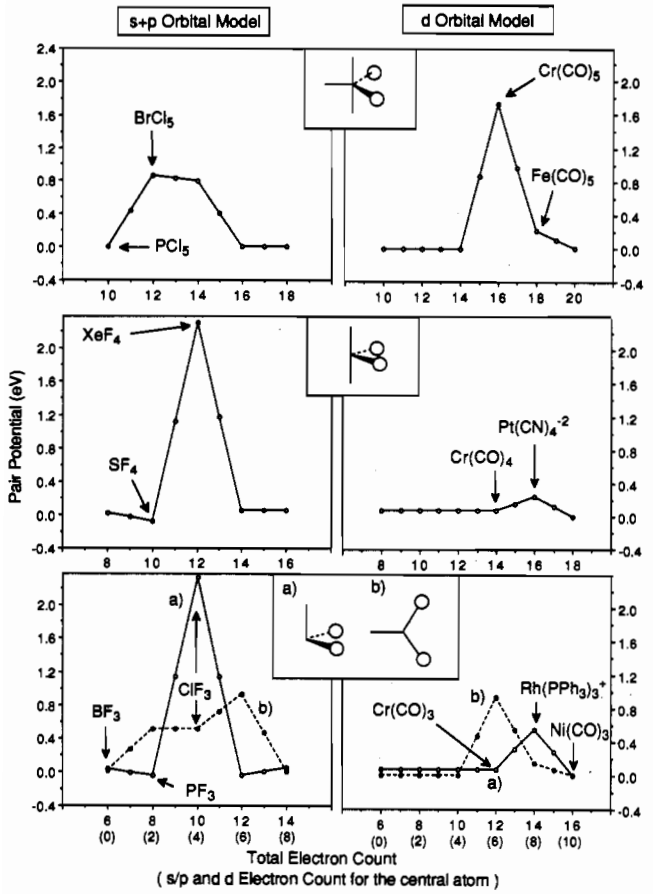

Figure 6. Calculated pair potentials of two cis ligands in molecules with structures shown in **2** as a function of electron count. Parenthesized values: electron counts for the A-centered non- and antibonding s+p and d orbitals.

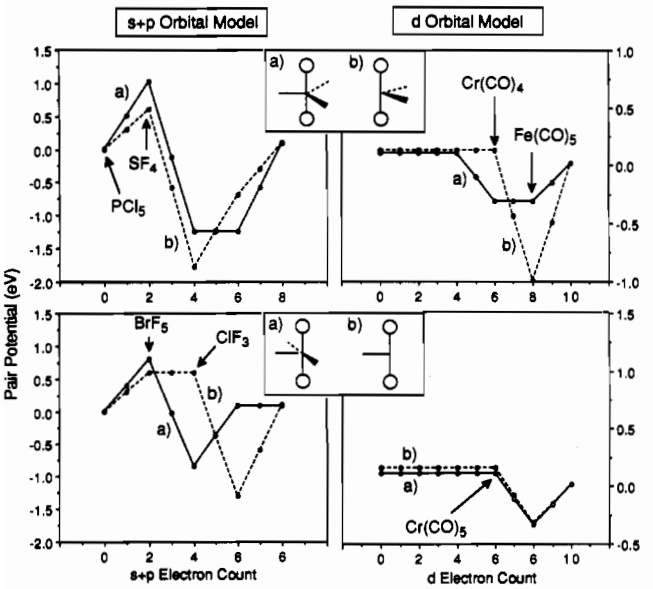

Figure 7. Calculated pair potentials of two trans ligands in molecules with structures shown in **2** as a function of electron count (cf. caption to Figure 6).

up in the plot. The reason for this certainly lies with our parameter choice. Using a series of different orbital parameters leads to a computed trans pair potential in accord with the calculated differences in bond overlap populations. For the d-orbital model for transition-metal complexes (Figure 7) we find that only minima occur for structures 1a, 2a, and 3b (**2**). This shortening of the axial bond lengths compared to the equatorial ones predicted by the model is observed in $Fe(CO)_5$ (axial 180.6 pm, equatorial (183.3 pm) although here, in comparison with experiment, we must be careful to separate the effects of σ and π bondong.[15]

For the T-shape structure, although the prediction of a longer unique M–L distance at d^8 is in accord with the computed bond overlap populations, it is contrary to the experimental result for the sole example, $Rh(PPh_3)_3^+$. However this molecule is distorted some way away from the ideal T in terms of L–M–L angles and contains a close phenyl group.

The predicted shorter axial than basal linkage for the d^6 square pyramid is matched by the relative sizes of the experimentally determined[16] vibrational force constants in $M(CO)_5$ molecules (M = Cr, Mo, W). Similarly, the predicted longer axial than equatorial bond in the d^6 butterfly structure, although small, is matched by the relative sizes of the experimentally determined[17] vibrational force constants in $M(CO)_4$ molecules. We should, however, note that the actual structures are distorted quite a bit away from this ideal "cis-divacant" structure. The non-zero value of the pair potential for d^0 and low d counts in these plots are results accessible from the angular overlap model. From d^0 to d^6 ϕ is simply equal to $1.75f_\sigma$ for the T and square-pyramidal geometries and equal to $4f_\sigma$ for the octahedral cis-divacant (butterfly) and trigonal-bipyramidal geometries.

Thus the relative bond lengths in these molecules, one of the two geometrical parameters accessible by using VSEPR ideas, may be viewed by using the same pair potential approach. Note that both main-group and transition-metal complexes fall under the same umbrella. In terms of an electron pair repulsion model, using the present approach, we would say that the relative bond lengths are set by the signs of the trans repulsions between bonding pairs of electrons. Contrast this with the VSEPR model, where the relative bond lengths in SF_4 and ClF_3, for example, are set by repulsions between bonded and nonbonded pairs.

The Jahn–Teller Theorem

As we pointed out in the Introduction, there is no monopoly on ways to approach the structural problem. However the ideas of the Jahn–Teller theorem have been of considerable importance in the understanding of transition-metal complexes. In this light, it is interesting to note that the peaks in the $\phi(x)$ plots often, but not always, correlate with points of first- and second-order Jahn–Teller instabilities. With reference to Figures 4 and 6, first-order instabilities are predicted to occur (Figure 8) for the trigonal bipyramid in I for d^5–d^7 (with a maximum at d^6) and in III and IV at d^7–d^9 (with a maximum at d^8) in IV there is a strong second-order coupling at d^6 that has a larger effect on $\phi(x)$ than the first-order one at d^8. The figure shows results for a d-orbital-only model. Clearly, the energy difference between the two levels that couple in the second-order Jahn–Teller distortion, one of which is of a_1 symmetry, will depend upon the inclusion of a central atom s orbital that transforms as the same symmetry species. Figure 9 shows how this pair potential is indeed sensitive to the s-orbital inclusion. When s and d orbitals are included on the central atom, the magnitudes of the pair potentials at d^6 and d^8 become quite similar.

For the main-group case, there is a first-order instability for the trigonal-planar to T-shape geometry in III for the 10-electron ClF_3. Using the p-orbital model for AH_2 in Figures 1 and 2, notice that there are accidental degeneracies at the bent geometry. The maxima in the pair potential correspond to those electron configurations where these degenerate orbitals are half full of electrons.

There is a very interesting result in II. The behavior in the pair potentials for d^7–d^9 (with a maximum at d^8) indicates, by analogy with the discussion above, that there might be a strong second-order coupling with a vibration mode which takes the butterfly structure to the square plane. However, the increase in the HOMO–LUMO gap at d^8 is generated purely by first-order changes in overlap; HOMO and LUMO remain of different

(15) Rossi, A. R.; Hoffmann, R. *Inorg. Chem.* **1975**, *14*, 365.
(16) Perutz, R.; Turner, J. J. *J. Am. Chem. Soc.* **1975**, *97*, 4791.
(17) Perutz, R.; Turner, J. J. *J. Am. Chem. Soc.* **1975**, *97*, 4800.

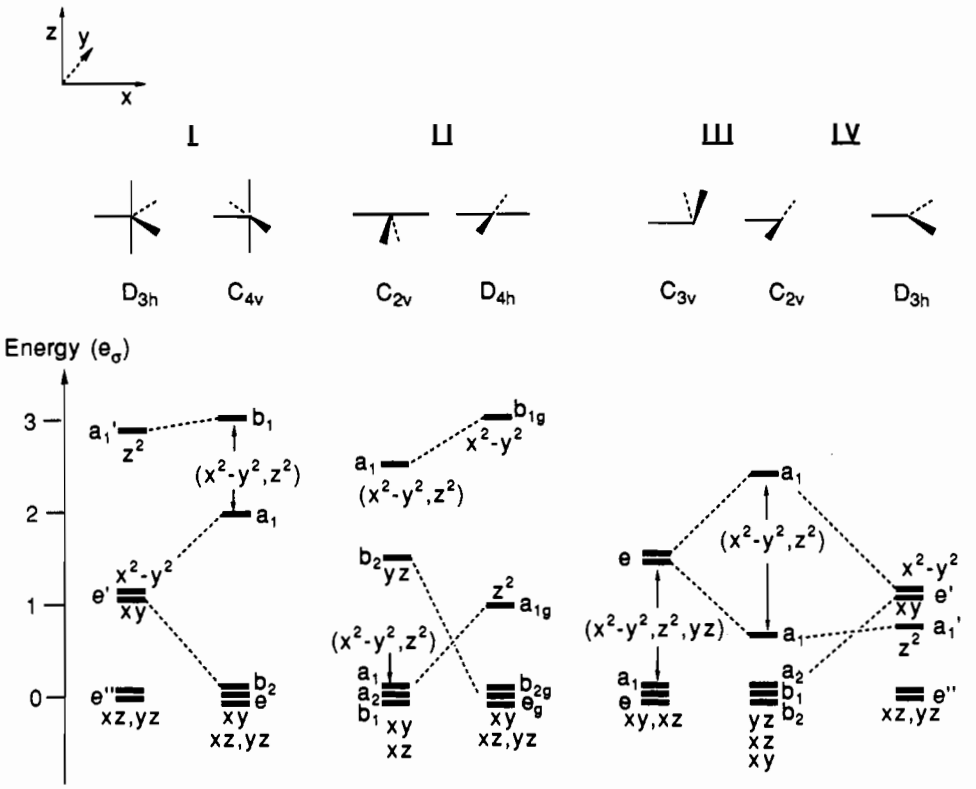

Figure 8. Molecular orbital diagrams for structures 1a–3c (**2**) using d orbitals only and constructed with the angular overlap approach.

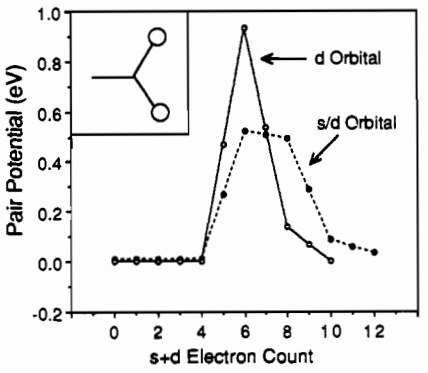

Figure 9. Pair potentials of two ligands of structure 3c using d orbitals and s+d orbitals for the central atom A, respectively, as a function of d-electron count.

symmetries. Thus, although the Jahn–Teller approach is a useful one in the prediction of molecular geometry, it is not applicable in all cases. Any opening of a gap on distortion though, whatever its origin, will give a positive pair potential at the relevant electron count.

The examples above used the pair potential to comment on the relative bond lengths in molecules where more than one symmetry-equivalent set is present. A molecule with octahedral symmetry and a d-electron count of d^7–d^9 is susceptible to a Jahn–Teller distortion, as indicated in **3**. Figure 10 shows the

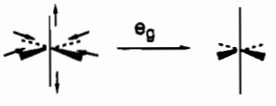

3

pair potential computed between two trans ligands for such an ideal octahedral complex (curve a). Certainly the plot does not indicate that such systems are geometrically unstable. It contains a region (d^0–d^6) where the pair potential is small and positive and a region up to d^{10} where it is zero. Both results are accessible from the angular overlap model. From d^0 to d^6 ϕ is simply equal to $4f_\sigma$. The zero value of the pair potential at higher electron

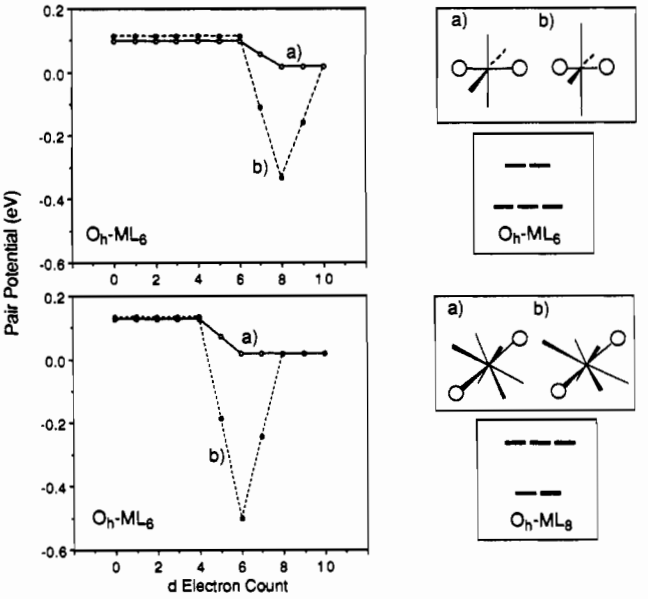

Figure 10. Calculated pair potentials of two trans ligands in O_h-ML_6 and ML_8 complexes using a d-orbital model. Shown are two curves, one (a) for the undistorted molecule and one (b) with a pair of elongated trans bonds.

counts is understandable from eq 2 and the energy levels[1] for the octahedron, square pyramid, and square. The highest energy orbital has identical energy ($3e_\sigma$–$9f_\sigma$ from the angular overlap model) in all three geometries. Conversion of the problem into a second-order one by stretching two trans linkages and computation of the pair potential between one pair of the remaining two leads straightaway to an attractive potential (curve b). The motion that such a result predicts is one component of the e_g vibration which leads to the classic Jahn–Teller distortions of d^7–d^9 ML_6 complexes. In more general terms the result may possibly be understood on symmetry grounds. All three pairs of trans linkages are symmetry equivalent, and thus elongation of one pair over another will not be seen in such a treatment. This is in contrast,

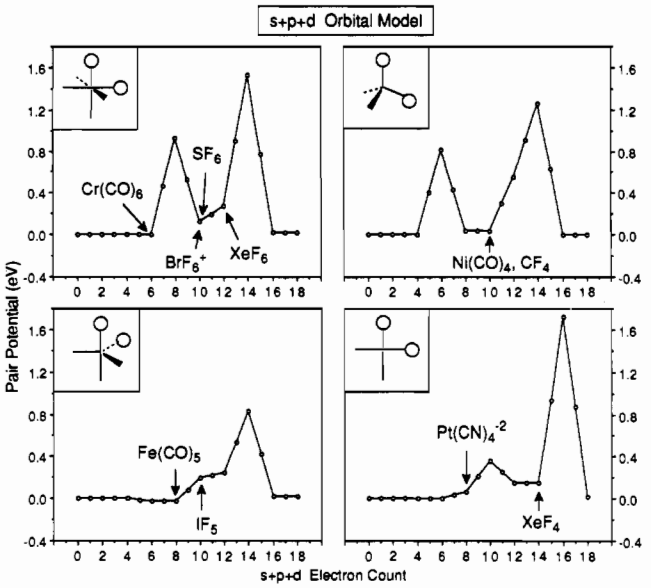

Figure 11. Calculated pair potentials of two cis ligands of O_h-ML_6, T_d-ML_4, D_{3h}-ML_5, and D_{4h}-ML_4 complexes using s+p+d orbitals for the central atom.

for example, to the non-zero pair potential between a pair of equatorial ligands in the trigonal-bipyramidal structure at d^6. Here the three ligands cannot be divided into mutually exclusive pairs. Support for such a symmetry argument comes from calculations on the ML_8 cube (Figure 10). An exactly analogous result is found for the ϕ parameter involving a pair of trans ligands here.

Electron-Counting Rules in Molecules and Clusters

Electron-counting rules such as the 8- and 18-electron rules for main-group and organometallic chemistry and Wade's rules[18] for clusters of both main-group and transition-metal types have proven enormously useful in providing a framework for the organization of chemistry. As we recently pointed out in the search for a similar rule for adsorption on surfaces,[19] use of the molecular pair potential provides another way to view rules such as these.

Figure 11 shows computed pair potential plots as a function of central atom electron count between two cis L groups in four standard geometries found for transition-metal ML_n species. We chose this pair potential since in all the geometries (with the exception of the tetrahedron) no stable geometry is expected to result by moving the ligands apart. If the amplitudes of the maxima found in $\phi(x)$ are larger than the metal–ligand bond energy, certain electron counts will lead to instabilities associated with ligand loss. For example, the pair potential would be so repulsive for the hypothetical 20-electron species (d^8) $Fe(CO)_6$ that one of the CO groups would be ejected from the molecule to give the stable 18-electron molecule $Fe(CO)_5$. Thus the electron count at the foot of such peaks is that appropriate for stability and leads to another way to view electron-counting rules of which the 8- and 18-electron rules are special cases. Notice that within the d region the highest electron counts allowed for the octahedron, trigonal bipyramid, and tetrahedron occur at d^6, d^8, and d^{10}, respectively. A similar picture holds for the square-planar geometry, but here the critical point on the plot corresponds to 16 electrons, i.e., d^8. The tetrahedral geometry is cleanly converted to the butterfly via repulsion of a pair of cis ligands. Notice that at d^6 this pair potential is largest, appropriate for the octahedral cis-divacant structure of $Cr(CO)_4$.

These calculations were performed by using standard parameters for transition metals and so are not immediately applicable to main-group molecules, but there are immediate indications of interesting structural results here too. The foot of the second peak of Figure 11 for the octahedron occurs at the filled d shell and represents the stability of main group molecules (e.g. SF_6 or BrF_6^+) with this geometry at the $(s+p)^0$ electron count. For the tetrahedron, stability is indicated by both 8- and 18-electron rules; i.e., d^{10} and $(s+p)^0$ electron counts occur at the same point. Thus although $S(e)F_6$ and CF_4 are stable octahedral and tetrahedral species, respectively, with an extra electron in each case the pair potential becomes repulsive. As a result, we expect to find a 7-valence-pair octahedral molecule AF_6^- which loses an F^- ligand to give stable square-pyramidal AF_5, in the same way that the hypothetical tetrahedral NF_4^- loses a ligand to give stable pyramidal NF_3. Notice the different behavior of the square-planar geometry. The plot predicts stability for the $(s+p)^4$ configuration. This is interestingly the appropriate electron count for the square-planar molecule XeF_4. The result for the trigonal bipyramid is not quite as clear. The d-orbital result predicts a maximum at d^{10}, but the s+p-orbital model, a value close to zero. What is actually seen is the sum of the two. A calculation where the d orbitals are contracted does in fact lead to a pair potential close to zero for the trigonal bipyramid. Thus the hypothetical trigonal-bipyramidal molecule SF_5^- loses an equatorial ligand to give stable butterfly SF_4.

The crucial role of the valence s orbital in determining the structure shows up nicely too. The hypothetical AF_6^- molecule, used in our illustration above, is isoelectronic with the stable species XeF_6 and BrF_6^-. Indeed, there is a whole series of octahedral or slightly distorted octahedral molecules with 7 valence pairs, the undistorted members of which are violators of the VSEPR rules.[20] Figure 11 shows the pair potential plot for the six-coordinate molecule using an s+p+d model, where at the relevant electron count there is a repulsive cis ligand pair potential. However, use of the angular overlap model (including both e_σ and f_σ terms) for the p-orbital manifold alone leads to a zero value for this pair potential for the 6-pair case (7 if the s-located pair is included). Thus the pair potential may run from being zero on the p-orbital-only model (where the s orbital is stereochemically impotent), giving an octahedral geometry with an inert pair, through small values to give the distorted octahedral geometry of XeF_6, to being large and leading to the ligand loss in (presently hypothetical) molecules such as IF_6^-. Such behavior may be mimicked by changing the parameters of the extended Hückel model to simulate such electronic requirements.

Similar considerations apply to the pair potential calculated for polynuclear molecules. These species are of two types, low-nuclearity molecules such as $Mn_2(CO)_{10}$ and $Fe_3(CO)_{12}$ and cage molecules such as $B_6H_6^{2-}$, although both types may often be accommodated in the widest view of Wade's rules. Figure 12 shows the pair potential calculated between two ligands in M_2L_{10} and M_2L_8 molecules. Notice that again there are two peaks. The d-electronic configuration corresponding to the foot of the first peak in Figure 11a is appropriate (d^7) for the stable molecule $Mn_2(CO)_{10}$ and in Figure 11b is appropriate (d^8) for the not-so-stable species $Fe_2(CO)_8$, isolobal with ethylene. The foot of the second peak corresponds to the state of affairs where there is a pair of central atom s/p electrons per M_2 unit plus a filled d shell. Such an electronic situation would be appropriate for the known species S_2F_{10} and unknown P_2F_8 species where the s/p pair of electrons is associated with the S–S and P–P bonds respectively.

As we know from orbital considerations,[21] the ML_n geometry is vital in determining the optimal number of electrons for stability. For example the trigonal bipyramid less one axial ligand and with a d^9 electron count is isolobal with CH_3 but the trigonal bipyramid less one equatorial ligand and with a d^8 electron count is isolobal with CH_2. Thus in Figure 12b,c the critical electron counts for two M_2L_8 geometries are 8 and 9, respectively. These correspond to the molecules $Fe_2(CO)_8$ and $Fe_2(CO)_8^{2-}$, respectively.[22]

(18) Wade, K. *Adv. Inorg. Chem. Radiochem.* **1976**, *18*, 1.
(19) Burdett, J. K.; Fässler, T. F. *Inorg. Chem.* **1990**, *29*, 4594.
(20) The recently determined structure of BrF_6^- shows an undistorted octahedral geometry as does BrF_6^+: Mahjoub, A. R.; Hoser, A.; Fuchs, J.; Seppelt, K. *Angew. Chem., Int. Ed. Engl.* **1989**, *101*, 1528. Further examples: Reference 1. Greenwood, N. N.; Earnshaw, A. *Chemistry of the Elements*; Pergamon Press: Oxford, U.K., 1984.
(21) Hoffmann, R. *Angew. Chem., Int. Ed. Engl.* **1982**, *21*, 711.
(22) The pair potentials in the staggered conformation observed for $Mn_2(CO)_{10}$ and $Fe_2(CO)_8^{2-}$ are virtually identical.

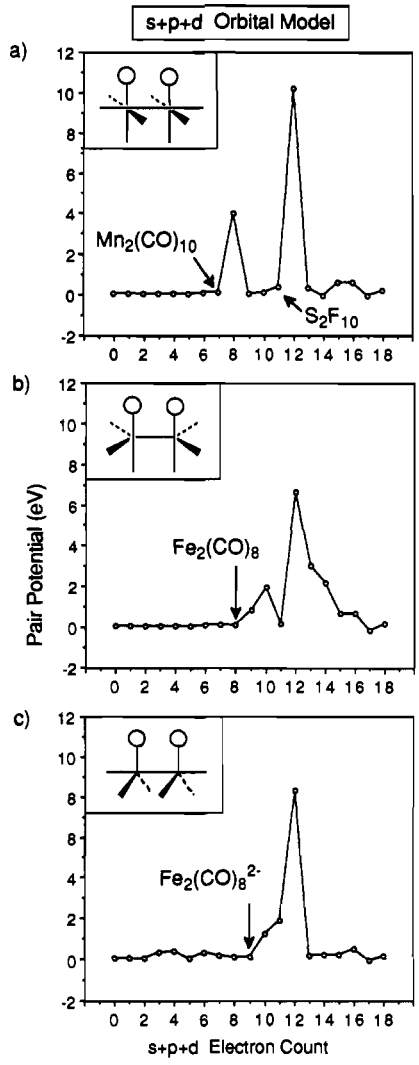

Figure 12. Calculated pair potentials of two cis ligands located at two adjacent atoms in M_2L_{10} and M_2L_8 as a function of s+p+d electron count of M.

Figure 13 shows cis and trans $\phi(x)$ plots between BH units in the octahedral cage molecule $B_6H_6^{2-}$. They show a sharp increase just above 26 electrons. Recall from Wade's rules that this molecule is stable for a total of 26 electrons, made up of 7 skeletal electron pairs plus 6 B–H bonding pairs. The positive cis potential has an interesting geometrical result. The strong repulsion at 28 electrons between a pair of adjacent BH units in the octahedral would lead to an opening an edge of this deltahedron. The result is a nido pentagonal bipyramid (**4**) which, from Wade's rules, is

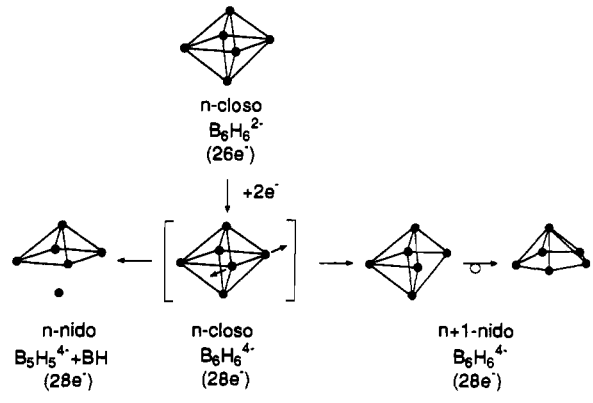

4

stable for an electron count of 28. Similar results apply to larger

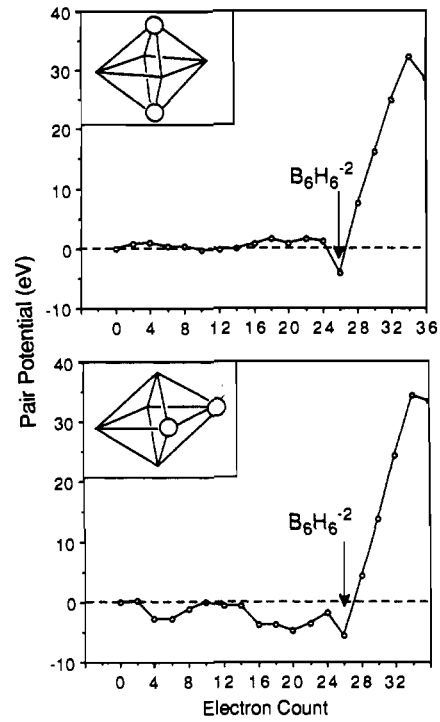

Figure 13. Calculated pair potentials of two BH units in (a) trans and (b) cis positions of an O_h-B_6H_6 cluster as a function of electron count.

deltahedra; in each case, the nido $(n + 1)$-vertex deltahedron can be generated via opening an edge of the closo n-vertex one. Alternatively, we could regard either the large repulsive cis or trans pair potential at 28 electrons as leading to conversion of $B_6H_6^{4-}$ (28 electrons) into $B_5H_5^{4-}$ (24 electrons) + BH. The 24-electron $B_5H_5^{4-}$ species would be stable as a nido octahedron.

One of the features of this plot is the negative pair potential at 26 electrons. This turns out to be controlled by the choice of coordination geometry for the B_2H_2 unit in the calculation of the energetics of $B_4H_4 + B_2H_2$, which contributes to the pair potential. The qualitative features of the variation of the pair potential is similar almost irrespective of this choice, but the amplitude at 26 electrons is largest for the case where B_2H_2 is modeled by two linked BH units as shown in Figure 13 and is less if the BH units are separated (this choice preserves the number of close B–B contacts in the computation of ϕ). Importantly, the vital feature of the plots, namely the sharp rise in the pair potential past 26 electrons, is maintained irrespective of this choice.

Discussion

We have indicated in this paper some useful aspects of the pair potential calculated between atoms in molecules. We reserve for Appendix I further discussion of some subtleties in its calculation. Fundamentally, knowledge of the sign and magnitude of $\phi(x)$ determines angular geometries, relative bond lengths, and critical electron counts for the electronic stability of molecules with certain structures. Our arguments are applicable to both main-group and transition-metal complexes. In the interests of generality, we have used a single set of orbital parameters to compute $\phi(x)$, but the use of specific parameters (e.g., use of those appropriate for P and F in computations on the PF_5 molecule) does in fact lead to a more detailed picture. One of the problems associated with such a generic model is that the magnitudes of the pair potentials are not very discriminatory. Thus, in our discussions on the AX_4 and ML_4 molecules it is not clear in numerical terms when an angular distortion will appear or a ligand be dissociated as the pair potential increases. However, the general trends are clear. For specific cases of course, more accurate calculations would be appropriate.

Our model only allows comment on the "repulsions" between "bond pairs" since we have no way to calculate the repulsion between lone pairs and between lone pairs and bonding pairs. In

Table II. Extended Hückel Parameters

valence orbital		H_{ii}, eV	ξ_1	ξ_2	c_1[a]	c_2[a]
Cr	3d	−11.22	4.95	1.8	0.506	0.675
	4s	−8.66	1.70			
	4p	−5.24	1.70			
B	2s	−15.20	1.30			
	2p	−8.50	1.30			
H	1s	−13.60	1.30 (2.425)[b]			

[a] Coefficients of the double-ξ function of the d orbitals. [b] An exponent of 2.425 was used in the calculations of all AX_n systems in order to reduce the ligand–ligand interaction as indicated above.

spite of this, the pair potential concept has led to the generation of the nearest thing so far to the VSEPR concept of repulsion between electron pairs located around a central atom. One rather interesting result of the approach is the influence of the stability of the ML_{n-2} and ML_{n-1} or AX_{n-2} and AX_{n-1} structures on that of ML_n and AX_n via the definition of the pair potential. The ML_n and AX_n molecules appear to have a "memory" of their genesis from smaller fragments that control their stability.

In more general terms, the form of the pair potential just rephrases the well-known rule that controls the structures of molecules; namely, species that are stable geometrically usually enjoy large HOMO–LUMO gaps. Behind such a statement lies the origin[1] of electron-counting rules (such as the 18-electron rule and Wade's rules), rules of the Walsh type, and the predictions of both first- and second-order Jahn–Teller effects. In all three areas, systems with small gaps will distort (or eject a ligand) to produce a molecule with a larger gap. Thus, we find by analysis of the computed energy levels as a function of geometry that the pair potential (effectively a force between unfavorably located ligands) can be tied directly to the opening of a gap and a stabilization of the HOMO on distortion. It has a maximum along a distortion coordinate when the HOMO–LUMO gap is smallest, and this is especially pronounced if there is an orbital crossing or touching which gives rise to an identity zero gap. Such a crossing will lead to either an "accidental" or symmetry-enforced degeneracy and a Jahn–Teller type of instability.

Acknowledgment. This research was supported by The University of Chicago. The stay of Thomas Fässler at Chicago was made possible by a generous stipend from the Deutsche Forschungsgemeinschaft. We wish to thank John Mitchell for many useful conversations.

Appendix I

The pair potential is a commonly used concept in surface chemistry. On a surface the adsorption of a single species is determined exclusively by the local properties of the adsorbate–surface interaction. Adsorption of a second atom or molecule induces a perturbation of the surface density of states. This adsorbate–adsorbate interaction is traditionally defined by a relevant set of pair potentials. The interactions can be through-space ones of the van der Waals, dipole–dipole or orbital overlap or via overlap interactions through the bond or band. These lateral interactions, usually in the range of 10^{-3}–0.5 eV, are much smaller of course than typical bond energies and are of the same magnitude as surface diffusion barriers. Quantum-mechanical, thermodynamic, and statistical methods may be coupled to such a pair potential description to study LEED structures, island formation, and the mixing/segregation problem in coadsorbed systems.

Using the same principles for molecules, calculation of the binding energy of one ligand or substituent (eq A1) with respect to a second ligand or substituent (eq A2) in a transition-metal complex or main-group molecule allows us to determine the through-bond interaction, the pair potential, ϕ, of two ligands or substituents in exactly the same way (eq A3).

bond energy of X with respect to fragment

$$BE_0 = E(AX) - E(A + X) = E(AX) - E(A) - E(X) \quad (A1)$$

bond energy of X with respect to fragment AY

$$BE_1 = E(AYX) - E(AY + X) = E(AYX) - E(AY) - E(X) \quad (A2)$$

interaction energy or pair potential, ϕ, between X and Y

$$\phi = BE_1 - BE_0 = [E(AYX) - E(AY) - E(X)] - [E(AX) - E(A) - E(X)] = [E(AYX) + E(A)] - [E(AX) + E(AY)] \quad (A3)$$

interaction energy for X = Y

$$\phi = [E(AX_2) + E(A)] - 2E(AX) \quad (A4)$$

example for two cis ligands in an octahedral complex ML_6

$$\phi = E(O_h\text{-}ML_6) + E(C_{2v}\text{-}ML_4) - 2E(C_{4v}\text{-}ML_5) \quad (A5)$$

This is shown pictorially in **5** and defines the symbolic representation of these pair potentials used in the figures in the body

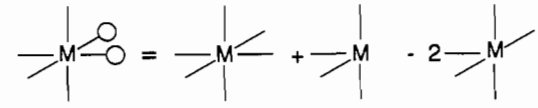

5

of the paper. We know that 1-electron methods to determine absolute bond energies are not very reliable, so the numbers calculated with eq A1 or A2 are not very usefl. On the other hand, in the calculation of the energy difference ϕ, where both terms in eq A3 or A4 have equal numbers of A–X and A–Y bonds, these approaches become much more viable.

Plotting the energy difference of two isomer structures as a function of the fractional orbital filling, x, allows a direct connection between the electronic structure and the topology of molecules or solids via the method of moments. The energy difference $\phi(x)$ may be viewed in a similar way, but with the difference that here the energies of three structures (A, AX, AX_2) are involved (four if X ≠ Y: A, AX, AY, AXY). Whereas the energetic comparison of two structures as a function of electron count provides no ambiguities, there are some questions to be answered for the present case of the calculation of ϕ.

To compare the energies of three (or more) structures as a function of fractional orbital filling, x, the same number of orbitals is required for each structure. This is only true in the nonreduced form of eq A3, where the systems A + 2X, AX + X, and AX_2, instead of A, AX, and AX_2, are compared. If the orbitals of X are energetically separated from the energy levels of the fragment A, all three terms of eq A4, involving AX_2, A, and AX, have the same number of A–X non- and antibonding orbitals (**6**). This

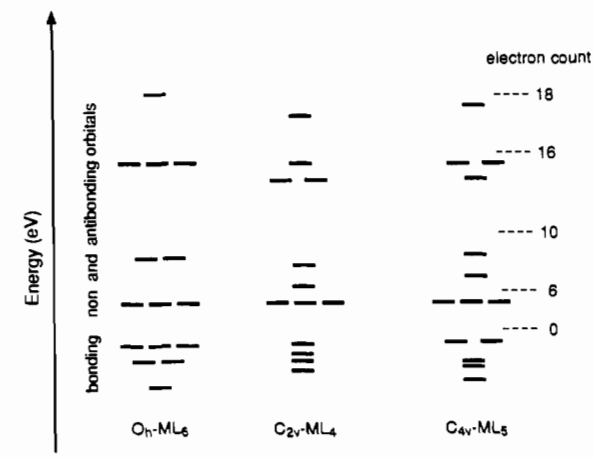

6

is the case in all complexes and molecules where X is a more electronegative ligand (substituent) than the central atom of fragment A to which the ligands are bound. These are usually also the chemically relevant orbitals, and it is often sufficient to compare the structures by starting with an electron count where all A-X bonding levels are already filled to avoid this problem. Even so, with more than two sets of energy levels the question does arise as to whether the enerties of the relevant structures should be compared at constant Fermi level or by ensuring that there are the same number of electrons in each structure to be compared. For the case of the two cis ligands of the octahedron, should then the properties of the merged density of states $[(O_h\text{-}ML_6) + (C_{2v}\text{-}ML_4)]$ be compared with the merged density of states $[2E(C_{4v}\text{-}ML_5)]$, or should the energies $E(O_h\text{-}ML_6)$, $E(C_{2v}\text{-}ML_4)$, and $2E(C_{4v}\text{-}ML_5)$ be separately evaluated at each electron count and then compared?

If the orbitals of the isolated ligand X lie energetically between the chemically important orbitals of the unit A or AX, the energy as a function of orbital filling has to be calculated for the case where the orbitals of the fragment A or AX are merged with the orbitals of the isolated ligand; otherwise, the pair potential exhibits wildly oscillating (and chemically meaningless) behavior in this region. This implies that $[E(AX + X)](x)$ or $[E(A + 2X)](x)$ has to be calculated instead of $[E(AX)](x)$ or $[E(A)](x)$. This is the case too for the pair potential between two vertices in the octahedral cluster B_6H_6 (here, A = C_{2v}-B_4H_4, X = BH). Here we need to calculate the pair potential as

$$\phi(x) = [E(B_6H_6)](x) + [E(B_4H_4 + 2BH)](x) - 2[E(B_5H_5 + BH)](x)$$

As discussed in the text, this is a case where the total number of close contacts is only maintained if two separated BH units are used in the second term.

Predictions from the method of moments as to the shapes expected for the $\phi(x)$ curves may sometimes be made. If two atoms first see each other via a self-returning walk of length 4, then the pair potential should exhibit four nodes, on the basis of the same type of argument employed for the energy difference plots themselves. Indeed, this expected correlation between $\Delta E(x)$ and $\phi(x)$ is found in Figure 1. However the sign of $\phi(x)$ may often not be as easily predicted. For the comparison of two densities of states, then the existing arguments show that the system with the larger fourth moment will be the more stable one for early and late orbital occupancies. But determination of $\phi(x)$ involves more than two sets of energy levels. If two merged sets of energy levels are used, then no ambiguity arises, but if three unmerged sets are used in the comparison, as we describe above, then the ideas associated with the moments method make no predictions as to the resultant sign of $\phi(x)$.

Appendix II

All calculations were performed by using the extended Hückel method. The parameters used are given in Table II. For the calculations of AX_n systems (Figures 4 and 6-10) Cr parameters for s/p, d, and s/p/d orbitals were used. To reduce the ligand-ligand interaction in these systems, the hydrogen Slater type orbital exponent was varied from 1.3 to 2.425 (the value used for fluorine 2s). Qualitatively similar results were obtained by using the standard parameters for H 1s and setting the ligand-ligand overlap integrals equal to zero. For the calculation shown in Figures 11-13 the usual Cr, H, and B parameters were used (Table II).

All central atom (A or M)-hydrogen distances were kept to 1.8 Å; for calculations involving M-M bonds a M-M distance of 2.49 Å was used. The B-B and B-H distances were 1.75 and 1.2 Å, respectively.

Contribution from the Department of Chemistry, University of Maine, Orono, Maine 04469, and Departments of Physics and Chemistry, Bowdoin College, Brunswick, Maine 04011

Photoluminescence and Electronic Structure of $Tl[Au(CN)_2]$: Evidence for Relativistic Effects in Thallium-Gold and Gold-Gold Interactions

Zerihun Assefa,[†] Frank DeStefano,[†] Mohammad A. Garepapaghi,[‡] Joseph H. LaCasce, Jr.,[‡] Steve Ouellette,[†] Michael R. Corson,[‡,§] Jeffrey K. Nagle,*[,∥] and Howard H. Patterson*[,†]

Received April 10, 1990

Experimental results of a study of the photoluminescence of microcrystalline $Tl[Au(CN)_2]$ as a function of temperature (1.7-400 K) and magnetic field (0-6 T) are described. These results, along with relativistically modified extended Hückel calculations, provide evidence that covalent Tl-Au interactions alter its spectroscopic properties in comparison with isostructural $Cs[Au(CN)_2]$. Specifically, the absorption and luminescence of $Tl[Au(CN)_2]$ appear at lower energies than for $Cs[Au(CN)_2]$, and a comparison of the luminescence spectra and lifetimes for the two compounds reveals evidence for an increased rate of intersystem crossing in $Tl[Au(CN)_2]$ relative to $Cs[Au(CN)_2]$. Both effects are reflective of covalent Tl-Au interactions in $Tl[Au(CN)_2]$. The electronic structure calculations clearly demonstrate the covalency of both the Tl-Au and Au-Au interactions in $Tl[Au(CN)_2]$ and reveal specific orbital contributions responsible for these interactions. Relativistic effects are shown to play an important role in the Tl-Au and Au-Au bonding.

Introduction

The tendency of certain 5d elements such as Ir, Pt, and Au to bond to 6p elements such as Tl and Pb in some compounds has recently been demonstrated.[1] It is likely that relativistic effects play an important role in this phenomenon by altering the energies and sizes of the valence orbitals involved as compared to the nonrelativistic situation.[1,2] X-ray structural analysis of single crystals has been invaluable in establishing the presence of such bonding,[3] but little is known about the detailed electronic structures of these compounds. Spectroscopic investigations, including both electronic absorption and luminescence, and electronic structure

[†] University of Maine.
[‡] Department of Physics, Bowdoin College.
[§] Present address: Physical Sciences, Inc., 603 King St., Alexandria, VA 22314.
[∥] Department of Chemistry, Bowdoin College.

(1) See for example Ziegler, T.; Nagle, J. K.; Snijders, J. G.; Baerends, E. J. *J. Am. Chem. Soc.* **1989**, *111*, 5631-5635 and references therein.
(2) (a) Pyykkö, P. *Chem. Rev.* **1988**, *88*, 563-594. (b) Pyykkö, P. In *Methods in Computational Chemistry*; Wilson, S., Ed.; Plenum Press: New York, 1988; Vol. 2, pp 137-221. (c) Schwerdtfeger, P.; Dolg, M.; Schwarz, G. A.; Bowmaker, W. H. E.; Boyd, P. D. W. *J. Chem. Phys.* **1989**, *91*, 1762-1774. (d) Ziegler, T.; Snijders, J. G.; Baerends, E. J. *J. Chem. Phys.* **1981**, *74*, 1271-1284. (e) Balasubramanian, K. *J. Phys. Chem.* **1989**, *93*, 6585-6596. (f) Pyykkö, P.; Desclaux, J.-P. *Acc. Chem. Res.* **1979**, *12*, 276-281. (g) Schwerdtfeger, P.; Boyd, P. D. W.; Bowmaker, G. A.; Mack, H. G.; Oberhammer, H. *J. Am. Chem. Soc.* **1989**, *111*, 15-23. (h) Schwerdtfeger, P.; Boyd, P. D. W.; Burrell, A. K.; Robinson, W. T.; Taylor, M. J. *Inorg. Chem.* **1990**, *29*, 3593-3597.
(3) Nagle, J. K.; Balch, A. L.; Olmstead, M. M. *J. Am. Chem. Soc.* **1988**, *110*, 319-321.

0020-1669/91/1330-2868$02.50/0